Inorg. Chem. **2003**, *42*, 7123–7128

Crystal Structure and Spectroscopic Characterization of $K_8(VO)_2O(SO_4)_6$

Søren B. Rasmussen,[†,‡] Rikke Mattsson Rasmussen,[†,‡] Rasmus Fehrmann,*[,†,‡] and Kurt Nielsen[‡]

ICAT (Interdisciplinary Research Center for Catalysis) and Department of Chemistry, Technical University of Denmark, DK-2800 Kgs. Lyngby, Denmark

Received May 19, 2003

Red and yellow dichroistic crystals of a vanadium(V) compound, potassium (μ-oxo, di-μ-sulfato)bis(oxodisulfatovanadate), $K_8(VO)_2O(SO_4)_6$, have been obtained from the ternary catalytic model melt system $K_2S_2O_7$–K_2SO_4–V_2O_5. By slow cooling of the melt from 420 to 355 °C, crystal growth occurred, using solid V_2O_5 crystals present in the melt as nucleation promoter. The compound crystallizes in the monoclinic space group $P2_1$ with $a = 13.60(9)$ Å, $b = 13.93(9)$ Å, $c = 14.05(9)$ Å, $\beta = 90.286(10)°$, and $Z = 2$. It contains two VO_6 octahedra linked together by a μ-oxo and two μ-sulfato bridges. Furthermore, each octahedron has two monodentate sulfate ligands, making the dimeric entity coordinatively saturated. IR spectroscopy shows bands arising from V—O—V and V═O stretches as well as splitting of sulfate bands due to the different degrees of freedom present for different conformations of sulfate ligands. The coordination of vanadium in $K_8(VO)_2O(SO_4)_6$ is discussed in relation to the reaction mechanism of SO_2 oxidation catalysis.

Introduction

In sulfuric acid production, which probably was the first major industrial use of a catalyzed process, the key step is the oxidation of SO_2 with O_2 to SO_3 by the contact process. In the last century, the vanadium based supported catalyst, promoted with alkali metal ions, became the preferred choice of catalyst. It is now generally accepted that the working catalyst is satisfactorily modeled by the $M_2S_2O_7$–M_2SO_4–V_2O_5/O_2–SO_2–SO_3–N_2 system[1] (M = Na, K, Rb, Cs) at 400–600 °C. The SO_2/SO_3 molar ratio, type of alkali metal ions, and temperature determine the oxidation state of vanadium in the mixture. At working temperatures, the active phase is a molten salt where vanadium oxosulfato complexes are formed. V(V) complexes of this type, especially the dimer $(VO)_2O(SO_4)_4^{4-}$, are regarded[1] as the catalytic active species. Vanadium complexes in the oxidation states +III and +IV are considered catalytically inactive.[2] Furthermore, the low solubilities of these complexes in the molten salt cause the well-known deactivation phenomena, where crystallization of V(III) and V(IV) salts occurs in the pore system of the solid kiselguhr carrier.[3] At around 480–500 °C, compounds with lower oxidation states (III and IV) decompose to SO_2 and compounds with vanadium in oxidation state +V. Upon further heating, the V(V) compounds release SO_3, and the melt will now correspond to a V_2O_5–M_2SO_4 molten salt system rather than the V_2O_5–$M_2S_2O_7$ type system, dominating the temperature region 400–500 °C. From the V_2O_5–$M_2S_2O_7$ system, the V(V) compounds[4,5] $Cs_4(VO)_2O(SO_4)_4$, $K_4(VO)_2O(SO_4)_4$, $Rb_4(VO)_2O(SO_4)_4$, and $CsVO_2SO_4$ have been isolated and their structures determined by single crystal X-ray investigations. The first three compounds exhibit discrete dimeric vanadium complexes even in the crystalline state, whereas $CsVO_2SO_4$ represents an entity in a polymeric network. High temperature investigations of the molten phase have shown that the dimeric compounds indeed exist as dimeric anions $(VO)_2O(SO_4)_4^{4-}$ in the molten phase and that $VO_2SO_4^-$ forms polymeric networks such as $(VO_2SO_4)_n^{n-}$. This proves that single crystal XRD is a powerful tool for acquiring information on the chemical and structural properties of the catalytic system. Glazyrin and co-workers[6] identified a sulfate rich compound, $K_3VO_2(SO_4)_2$, which was stable in the molten phase up to 620 °C. Other high

* Corresponding author. E-mail: rf@kemi.dtu.dk. Fax: +45 45883136.
† ICAT.
‡ Department of Chemistry.

(1) Lapina, O. B.; Bal'zhinimaev, B. S.; Boghosian, S.; Eriksen, K. M.; Fehrmann, R. *Catal. Today* **1999**, *51*, 469.
(2) Boreskov, G. K.; Polyakova, G. M.; Ivanov, A. A.; Mastikhin, V. M. *Dokl. Akad. Nauk SSSR*, **1973**, *210*, 626; *Dokl. Akad. Nauk SSSR* (Engl. Transl.) **1973**, *210*, 423.
(3) Boghosian, S.; Fehrmann, R.; Bjerrum, N. J.; Papatheodorou, G. N. *J. Catal*. **1989**, *119*, 121.
(4) Nielsen, K.; Fehrmann, R.; Eriksen, K. M. *Inorg. Chem.* **1993**, *32*, 4825.
(5) Rasmussen, S. B.; Eriksen, K. M.; Fehrmann, R.; Nielsen, K. Work in progress.
(6) Glazyrin, M. P.; Krasilnikov, V. N.; Ivakin, A. A. *Russ. J. Inorg. Chem.* **1981**, *26*, 1436.

10.1021/ic0301674 CCC: $25.00
Published on Web 10/02/2003

temperature work[7,8] on reactions between $(VO)_2O(SO_4)_4^{4-}$ and SO_4^{2-} in the molten phase have shown that at 450−470 °C sulfate breaks up the oxygen μ-oxo bridge of the dimer and forms two monomeric $VO_2(SO_4)_2^{3-}$ complexes. The stability of this complex in a wide temperature range is remarkable. Glazyrin and co-workers also proposed a number of compounds,[6,9] as various alkali salts, with stoichiometry equal to MVO_2SO_4, $M_4(VO_2)_2(SO_4)_2S_2O_7$, $M_2VO(SO_4)_3$, $MVO(SO_4)_2$, and $M_3VO_2(SO_4)_2$. However, no structural determinations of the compounds were achieved, but it was possible to index the X-ray diffraction patterns. Later, all of the above-mentioned compounds, except for $M_3VO_2(SO_4)_2$, have been determined to have the indicated stoichiometric compositions, though some of them have structural properties different from those proposed by Glazyrin and co-workers. In this work, a compound, unexpected in this system, $K_8(VO)_2O(SO_4)_6$, has been identified. Structurally, it resembles the dimeric compounds $M_4(VO)_2O(SO_4)_4$, but the two extra sulfate ligands alter the chelating of sulfate in such a way that the catalytic activity of this particular compound must be low. However, information on ligand exchange in the catalytically active $(VO)_2O(SO_4)_4^{4-}$ complex might be obtained by comparing the structures of the compounds. This can be used for considerations of the molecular geometry of an intermediate complex in the catalytic cycle with coordinated SO_3. This could help to explain how the "coordinatively unsaturated sites"[10] of the supposed catalytic active dimeric complex coordinate the reactants SO_2 and O_2.

Experimental Procedures

Chemicals. Potassium pyrosulfate ($K_2S_2O_7$), was obtained from thermal decomposition of commercial $K_2S_2O_8$ (Merck pro analysi) as previously described.[3] Commercial potassium sulfate (K_2SO_4, Merck pro analysi) and vanadium pentoxide (V_2O_5, Cerac >99.99 pure) were used after drying at 120 °C. All handling of chemicals and filling and sealing of ampules were performed in a drybox with a H_2O content less than around 10 ppm. The samples were sealed in 0.5 atm O_2 (99.8% O_2 + 0.2% N_2 and Ar).

Synthesis of $K_8(VO)_2O(SO_4)_6$. Single crystals for X-ray diffraction analysis were obtained by mixing 11.7 g of $K_2S_2O_7$, 4.2 g of K_2SO_4, and 5.2 g of V_2O_5 yielding the molar relationship $4K_2S_2O_7 \cdot 1K_2SO_4 \cdot 1V_2O_5$. Mixing was done in the drybox, and the sample was transferred to a Pyrex ampule and afterwards sealed under 0.5 atm O_2. The ampule was inserted in a two zone glass furnace and positioned such that the neck of the ampule was in one zone while the body rested in the second zone. The body was equilibrated at 420 °C. This allowed for a temperature gradient across the ampule, keeping the remains in the neck as solids at 335 °C. This promoted crystal formation in the subcooled part of the melt. After equilibration for 2 h, the set-point of the high-temperature zone was decreased to 365 °C, just above the expected liquidus point. The furnace was cooled to 355 °C in 5 h, and crystallization occurred around 357 °C. The resulting sample was a mixture of glasses and some crystals. The crystals exhibited dichroism, as they were yellow from one side and red from the other. A crystal with the dimensions 0.10 mm × 0.075 mm × 0.045 mm was selected for single crystal X-ray diffraction.

Table 1. Crystallographic Data for $K_8(VO)_2O(SO_4)_6$[a]

chemical formula $K_8(VO)_2O(SO_4)_6$	fw 1039.04 g·mol L^{-1}
$a = 13.5973(9)$ Å	space group $P2_1$ (No. 4)
$b = 13.9288(9)$ Å	$T = 25$ °C
$c = 14.0516(9)$ Å	$\lambda = 0.71073$ Å
$\beta = 90.2860(10)°$	$\rho_{calcd} = 1.297$ g cm^{-3}
$V = 2661.3(3)$ Å^3	$R_1 = 0.0772$ (0.0417)[b]
$Z = 2$	$R_2 = 0.0859$ (0.0749)[c]

[a] R-values in parentheses refer to observed reflections only [$I > 4\sigma(I)$]. [b] $R_1 = \sum||F_o| - |F_c||/\sum|F_o|$. [c] $R_2 = (\sum_w||F_o^2 - F_c^2|^2/\sum_w|F_o^2|^2)^{1/2}$.

A powder sample was prepared for IR spectroscopy and TGA/DTA measurements. The ampule contained the exact stoichiometric composition, known from the X-ray analysis, of the compound, i.e., $2K_2S_2O_7 \cdot 2K_2SO_4 \cdot V_2O_5$, and was kept for 3 days at 350 °C after equilibration at 420 °C. A minor amount of remaining liquid, probably due to weighing uncertainties, was separated from the solid phase. After slow cooling to room temperature, the ampule was cut open in the drybox, and the solid phase was extracted and used for IR spectroscopy and TGA/DTA. Visual inspection of the crystals in a microscope confirmed that the sample indeed contained the same type of yellow/red crystals as the single crystal used for XRD. Large parts of the sample, however, were dark red amorphous material.

X-ray Diffraction. X-ray diffraction data were collected at room temperature on a Siemens SMART diffractometer using Mo Kα ($\lambda = 0.71073$Å) monochromatic radiation. Unit cell dimensions were refined and intensity data reduced by SAINT. The structure was solved by direct methods and refined in the space group $P2_1$ including full-matrix least-squares fitting of positional and anisotropic thermal parameters.[11,12] Data were calculated with atomic scattering factors and anomalous dispersion corrections obtained from SHELXTL.[11] Correction for absorption was performed by the Siemens SADABS program. Structure drawings were made using the ORTEP-III[13] thermal ellipsoid plot software.

IR Spectroscopy. The IR spectrum was recorded on a Perkin-Elmer 1710 infrared Fourier transform spectrometer at room temperature from the mixed polycrystalline and amorphous sample. The sample was ground in dry KBr (1 mg of sample in 100 mg of KBr) and pressed into a transparent disk. Transmittance was recorded against a KBr disk. Spectral resolution was around 4 cm^{-1}.

Thermogravimetric Analysis. A 331.2 mg sample was taken from the ampule and put into an alumina crucible. The sample was kept dry with a flow of dry air passing continuously through the compartment. The analysis was performed from 25 to 800 °C at a rate of 5 °C/min measured against an empty alumina crucible as reference.

Results and Discussion

Table 1 shows the crystal data for $K_8(VO)_2O(SO_4)_6$, while the bond lengths and bond angles are given in Tables 2 and 3, respectively. Thermal anisotropic parameters can be obtained from the supporting material.

(7) Rasmussen, S. B.; Eriksen, K. M.; Fehrmann, R. *J. Phys. Chem. B* **1999**, *103*, 11282.
(8) Boghosian, S.; Borup, F.; Chrissanthopoulos, A. *Catal. Lett.* **1997**, *48*, 145.
(9) Krasilnikov, V. N.; Glazyrin, M. P.; Ivakin, A. A. *Russ. J. Inorg. Chem.* **1980**, *25*, 1843.
(10) Bal'zhinimaev, B. S.; Ivanov, A. A.; Lapina, O. B.; Mastikhin, V. M.; Zamaraev, K. I. *Faraday Discuss. Chem. Soc.* **1989**, 133.
(11) Sheldrick, G. M. *Acta Crystallogr., Sect. A* **1990**, *46*, 467.
(12) Sheldrick, G. M. *SHELX 97, Program for the Refinement of Crystal Structures*; University of Göttingen: Göttingen, Germany, 1997.
(13) Burnett, M. N.; Johnson, C. K. *ORTEP-III: Oak Ridge Thermal Ellipsoid Plot Program for Crystal Structure Illustrations*; Report ORNL-6895; Oak Ridge National Laboratory: Oak Ridge, TN, 1996.

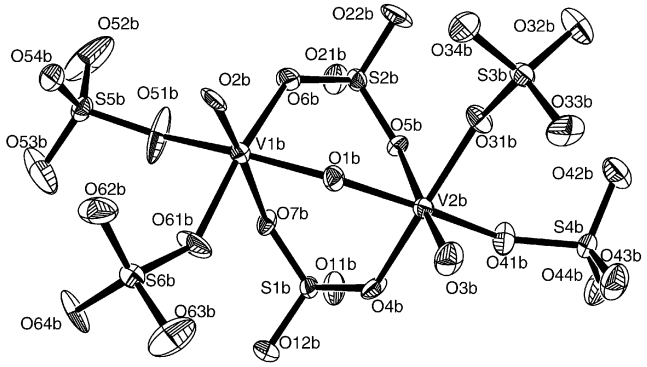

Figure 1. ORTEP-III plot of molecule B in the structure of $K_8(VO)_2O(SO_4)_6$. Molecule B corresponds to $^1/_2$ of the unit cell; cations (K^+) are omitted for clarity. Ellipsoids are plotted at the 50% probability level.

Table 2. Bond Lengths in $K_8(VO)_2O(SO_4)_8$ (in Å)

molecule A		molecule B	
V1A−O2A	1.571(7)	V1B−O2B	1.567(7)
V2A−O3A	1.601(6)	V2B−O3B	1.584(7)
V1A−O1A	1.782(6)	V1B−O1B	1.812(7)
V2A−O1A	1.801(7)	V2B−O1B	1.773(7)
V1A−O7A	2.281(7)	V1B−O7B	2.214(6)
V2A−O5A	2.209(6)	V2B−O5B	2.179(6)
V2A−O4A	1.964(6)	V2B−O4B	2.003(7)
V1A−O6A	1.981(7)	V1B−O6B	2.002(7)
V1A−O51A	1.939(6)	V1B−O51B	1.909(7)
V1A−O61A	1.922(7)	V1B−O61B	1.895(7)
V2A−O31A	1.895(6)	V2B−O31B	1.892(7)
V2A−O41A	1.953(6)	V2B−O41B	1.975(6)
O4A−S1A	1.525(6)	O4B−S1B	1.514(6)
O7A−S1A	1.454(6)	O7B−S1B	1.467(6)
O5A−S2A	1.465(6)	O5B−S2B	1.484(6)
O6A−S2A	1.489(6)	O6B−S2B	1.518(6)
S1A−O11A	1.464(6)	S1B−O11B	1.457(7)
S1A−O12A	1.445(7)	S1B−O12B	1.464(7)
S2A−O21A	1.447(7)	S2B−O21B	1.442(7)
S2A−O22A	1.444(7)	S2B−O22B	1.448(7)
S3A−O31A	1.553(7)	S3B−O31B	1.527(6)
S3A−O32A	1.449(6)	S3B−O32B	1.458(7)
S3A−O33A	1.434(7)	S3B−O33B	1.441(7)
S3A−O34A	1.412(7)	S3B−O34B	1.435(7)
S4A−O41A	1.526(6)	S4B−O41B	1.522(6)
S4A−O42A	1.452(7)	S4B−O42B	1.452(7)
S4A−O43A	1.444(8)	S4B−O43B	1.450(7)
S4A−O44A	1.431(7)	S4B−O44B	1.434(7)
S5A−O51A	1.544(6)	S5B−O51B	1.501(7)
S5A−O52A	1.462(7)	S5B−O52B	1.420(8)
S5A−O53A	1.461(7)	S5B−O53B	1.455(8)
S5A−O54A	1.442(7)	S5B−O54B	1.456(7)
S6A−O61A	1.516(6)	S6B−O61B	1.520(7)
S6A−O62A	1.442(7)	S6B−O62B	1.442(7)
S6A−O63A	1.444(8)	S6B−O63B	1.446(8)
S6A−O64A	1.449(7)	S6B−O64B	1.447(7)

Description of the Crystal Structure. The unit cell contains two discrete $(VO)_2O(SO_4)_6^{8-}$ ions (A and B), with the geometric arrangement of molecule B shown in Figure 1. Each ion contains two V atoms with distorted octahedral coordination. There are one μ-oxo and two μ-sulfato bridges between the two vanadium atoms in each molecule. Contrary to the $Cs_4(VO)_2O(SO_4)_4$ structure,[4] no bidentate chelate ligands are present. The bridging SO_4^{2-} ions are also observed for the mixed valence V(V)−V(IV) compound $K_6(VO)_4(SO_4)_8$[14] which has no μ-oxo bridge. The geometry with all together three bridges has previously been observed[15] in a polymeric compound of joint $(VO)_2O(SO_4)_2$ units. The terminal sulfates in $(VO)_2O(SO_4)_6^{8-}$ are unidentate coordinated to the vanadium atoms. Thus, it seems that the dimer,[4] $(VO)_2O(SO_4)_4^{4-}$, in the molten phase is able to coordinate sulfate further and remain as a discrete entity, before breaking up into monomers in the form of $VO_2(SO_4)_2^{3-}$. This has been shown to occur at 450−470 °C.[7,8]

Table 3. Selected Bond Angles in $K_8(VO)_2O(SO_4)_8$ (in deg)

molecule A		molecule B	
V1A−O1A−V2A	148.0(3)	V2B−O1B−V1B	144.7(3)
O1A−V1A−O6A	89.7(3)	O1B−V1B−O6B	88.3(3)
O1A−V1A−O7A	85.8(3)	O1B−V1B−O7B	85.4(2)
O1A−V1A−O51A	162.3(3)	O1B−V1B−O51B	163.8(3)
O1A−V1A−O61A	91.9(3)	O1B−V1B−O61B	93.2(3)
O1A−V2A−O4A	88.7(3)	O1B−V2B−O4B	89.2(3)
O1A−V2A−O5A	83.7(3)	O1B−V2B−O5B	86.2(3)
O1A−V2A−O31A	95.0(3)	O1B−V2B−O31B	98.9(3)
O1A−V2A−O41A	162.1(3)	O1B−V2B−O41B	163.6(3)
O2A−V1A−O1A	99.1(3)	O2B−V1B−O1B	97.7(3)
O2A−V1A−O6A	99.7(4)	O2B−V1B−O6B	99.7(3)
O2A−V1A−O7A	175.0(3)	O2B−V1B−O7B	176.5(3)
O2A−V1A−O51A	98.3(3)	O2B−V1B−O51B	97.9(3)
O2A−V1A−O61A	97.7(4)	O2B−V1B−O61B	96.8(3)
O3A−V2A−O1A	98.4(3)	O3B−V2B−O1B	97.3(3)
O3A−V2A−O4A	96.0(3)	O3B−V2B−O4B	97.3(3)
O3A−V2A−O5A	177.6(3)	O3B−V2B−O5B	176.4(3)
O3A−V2A−O31A	94.6(3)	O3B−V2B−O31B	98.4(3)
O3A−V2A−O41A	98.3(3)	O3B−V2B−O41B	96.5(3)
O6A−V1A−O7A	81.4(3)	O6B−V1B−O7B	81.8(3)
O61A−V1A−O6A	162.1(3)	O61B−V1B−O6B	163.1(3)
O61A−V1A−O7A	80.9(3)	O61B−V1B−O7B	81.5(3)
O61A−V1A−O51A	88.9(3)	O61B−V1B−O51B	89.2(4)
O51A−V1A−O6A	84.2(3)	O51B−V1B−O6B	84.9(3)
O51A−V1A−O7A	76.9(3)	O51B−V1B−O7B	79.1(3)
O4A−V2A−O5A	82.9(3)	O4B−V2B−O5B	83.4(3)
O31A−V2A−O4A	168.1(3)	O31B−V2B−O4B	161.3(3)
O31A−V2A−O5A	86.4(3)	O41B−V2B−O5B	80.2(3)
O31A−V2A−O41A	90.0(3)	O31B−V2B−O41B	87.9(3)
O41A−V2A−O4A	83.2(3)	O41B−V2B−O4B	80.2(3)
O41A−V2A−O5A	79.5(2)	O31B−V2B−O5B	80.3(3)
S1A−O4A−V2A	132.5(4)	S1B−O4B−V2B	132.2(4)
S1A−O7A−V1A	129.6(4)	S1B−O7B−V1B	133.0(4)
S2A−O5A−V2A	134.9(4)	S2B−O5B−V2B	131.1(4)
S2A−O6A−V1A	139.7(4)	S2B−O6B−V1B	133.4(4)
O4A−S1A−O7A	108.1(4)	O4B−S1B−O7B	109.6(4)
O5A−S2A−O6A	110.1(4)	O5B−S2B−O6B	109.9(4)

In comparison with other known compounds[4] containing the $(VO)_2O$ unit, the angle of the V−O−V bridge found here to be 145−148° for the A and B molecules of $K_8(VO)_2O(SO_4)_6$ is the smallest reported. It is however close to the 148.4° found for $(VO)_2O(SO_4)_2$, the only other known V(V)−O−V(V) compound with bridging sulfate groups. The O−S−O angles of the coordinated part of these bridging sulfate groups in molecules A and B are in the range 108.1−110.1° very close to the ideal tetrahedral angle of 109°. Thus, in order to maintain this almost ideal tetrahedral angle of the sulfate groups involved in bridging the two V(V) atoms, the V−O−V angle has to decrease compared to the other known structures without bidentate bridging sulfate ligands.

Three of the four oxygens bonded to S5b, the central atom of one of the terminal unidentate sulfate ligands, have rather large anisotropic displacement parameters, and this anisotropy cannot be refined satisfactorily by splitting the three

(14) Eriksen, K. M.; Nielsen, K.; Fehrmann, R. *Inorg. Chem.* **1996**, *35*, 480.

(15) Richter, K.-L.; Mattes, R. *Z. Anorg. Allg. Chem.* **1992**, *611*, 158.

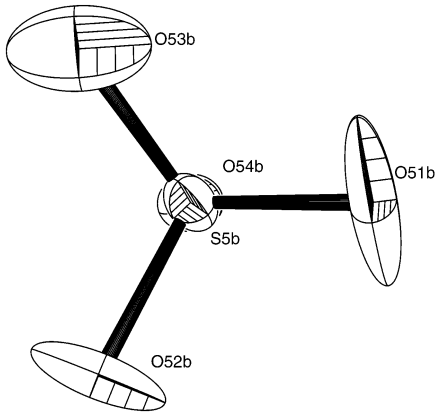

Figure 2. Plot of the terminal S5b−sulfate ligand. Displacement parameters illustrate the ligand rotation around the axis spanned by the 054b−S5b bond.

atoms. This can be seen in Figure 2, as an oscillation of the three atoms around the S5b−O54b bond. It is remarkable that the oxygen (O51b), bonded to V1b, participates in this oscillation. As described in the following subsection, the phenomenon is also observed in the IR spectrum of the powder sample.

An ORTEP-III stereo plot of the crystal packing in $K_8(VO)_2O(SO_4)_6$ is shown in Figure 3.

IR Spectroscopy. The IR spectrum of $K_8(VO)_2O(SO_4)_6$ is shown in Figure 4, and assignments of the bands are shown in Table 4. According to the empirical relationship[16] $\nu_{\text{stretch}} = 21349e^{-1.9176R} \pm 23$ cm^{-1}, the V=O stretches should be found at 1056, 1049, 1023, and 991 cm^{-1} for the observed bond lengths, R (in Å). V2a is present at 983 cm^{-1} which agrees well with the calculated 991 cm^{-1}. It is reasonable to suggest that V1b, V2a, and V2b overlap around 1050 cm^{-1} with a shoulder at 1036 cm^{-1}. The broad band at 718 cm^{-1} is due to the two μ-oxo bridges (V−O−V) in the unit cell. Other contributions to the IR spectrum from vanadium would probably be V−O−S vibrations at energies below 450 cm^{-1}. There are two significantly different types of sulfates present in the structure. Four unidentate SO_4^{2-} (V−SO_4) in each molecule and two bridging (V−SO_4−V). Coordination decreases the symmetry of sulfate from T_d to C_{3v} in the case of V−SO_4, and to C_{2v} in the case of V−SO_4−V. For C_{3v}, ν_3 and ν_4 will each split into two contributions. For C_{2v}, each ν_3 and ν_4 splits into three bands. The general decrease of symmetry makes ν_1 and ν_2 IR-active, while all four bands of uncoordinated SO_4^{2-} only can be seen by Raman spectroscopy. In the spectral range 1230−1050 cm^{-1}, six main bands can be found and ascribed to ν_3 modes. The three at highest energy, i.e., 1226, 1218, and 1199 cm^{-1}, probably originate from the bridging sulfate ligands while the bands at 1186, 1073, and 1061 cm^{-1} are assigned to ν_3 of unidentately coordinated sulfates. The ν_1 bands from bridging sulfate ligands are found at 972 and at 925 cm^{-1} for unidentate sulfate. At 905 and 882 cm^{-1}, relatively broad bands are seen. These are believed to originate from the long S−O bond of each sulfate ligand, as described by Mattes and Richter.[15] The two ν_4 bands from the bridging sulfate ligands appear at 667 cm^{-1} with a shoulder at 652 cm^{-1}. For the unidentate ligands, the ν_4 bands are seen at 595 cm^{-1} with a shoulder at 619 cm^{-1}. The ν_2 bands for bridging and

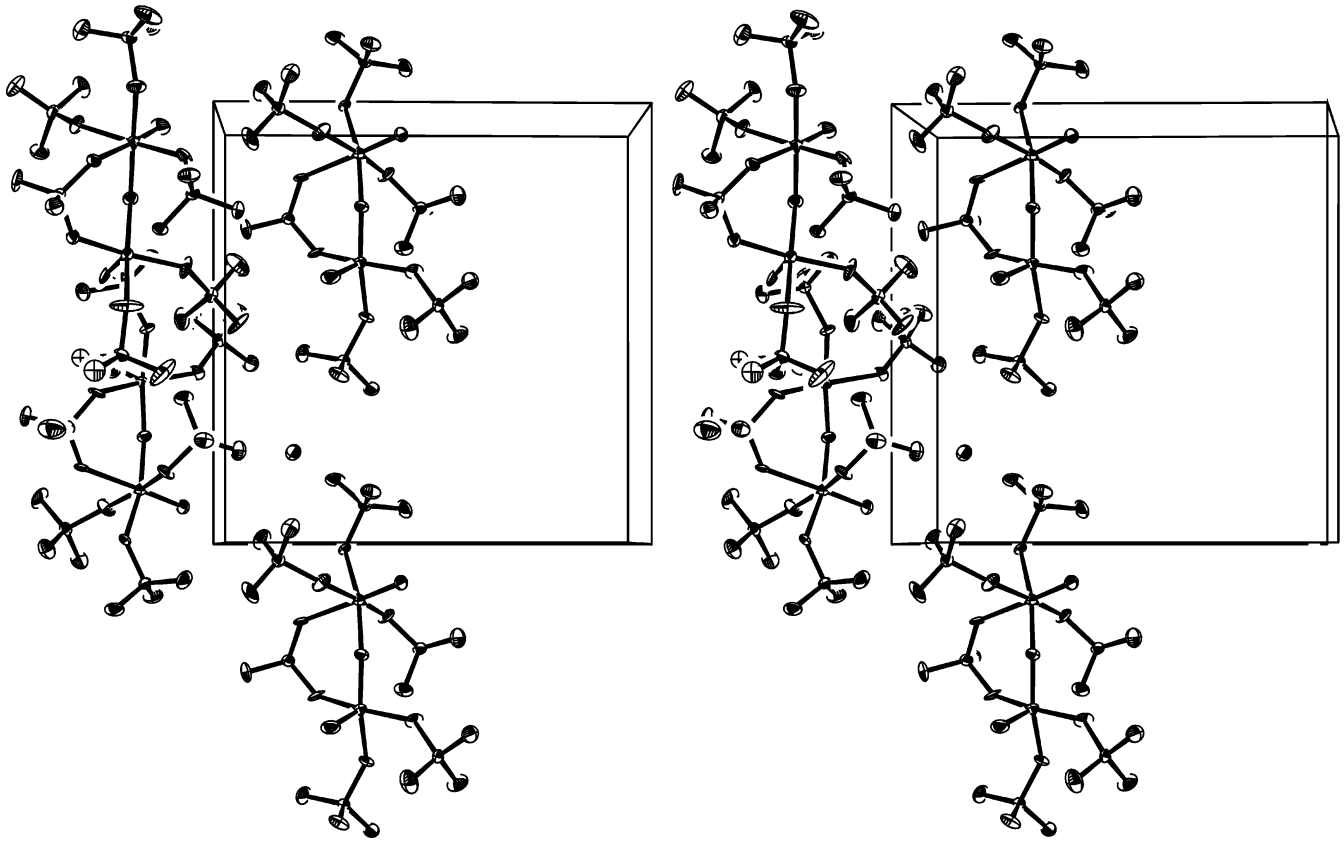

Figure 3. ORTEP-III stereo plot of $K_8(VO)_2O(SO_4)_6$.

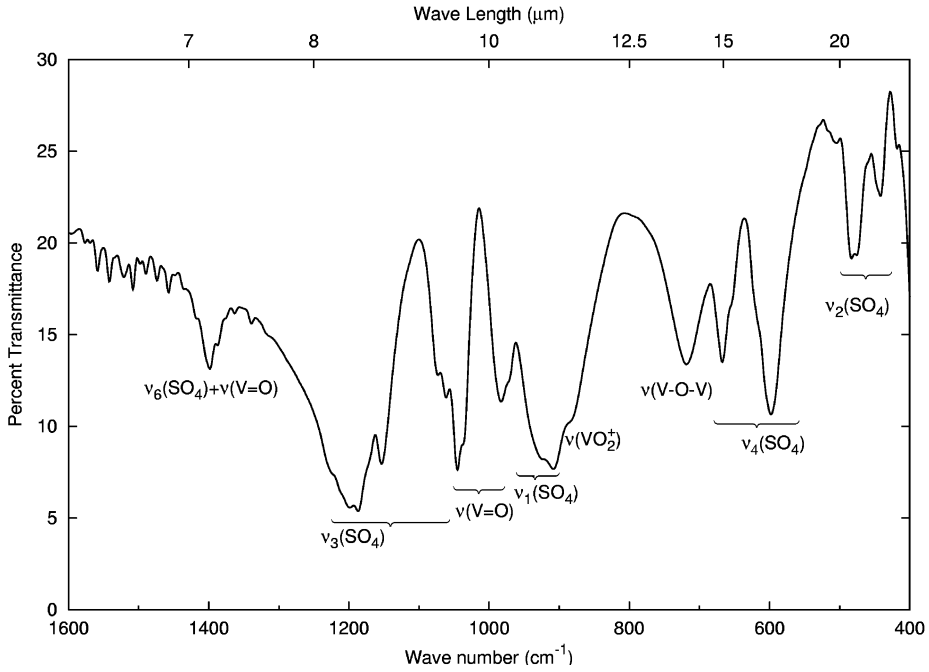

Figure 4. Infrared spectra of $K_8(VO)_2O(SO_4)_6$. See Table 4 for detailed assignment of bands.

Table 4. Infrared Bands (cm^{-1}) of $K_8(VO)_2O(SO_4)_6$ and Their Tentative Assignments

assignment	bands, (cm^{-1})
ν_3(V−SO_4−V)	1226, 1218, 1199, 1186
ν_3(V−SO_4)	1170, 1152, 1073, 1061
ν(V═O)	1045, 1036, 983
ν_1(V−SO_4−V)	972
ν_1(V−SO_4)	925
ν(S···O)	905, 882
ν(V−O−V)	718
ν_4(V−SO_4)	619, 652
ν_4(V−SO_4−V)	667, 652
ν_2(V−SO_4−V)	474
ν_2(V−SO_4)	440
$\nu_6(SO_4) + \nu$(V═O)[a]	1398

[a] Combination band. $\nu_6(SO_4)$ is probably around 250−350 cm^{-1}, see text.

unidentate sulfate ligands appear at 474 and 440 cm^{-1}, respectively. Finally, at 1398 cm^{-1} a combination band is seen. It is unlikely that any internal modes for either sulfate or vanadium should appear in this region. This is probably a combination band, which can appear when a single photon excites two vibrations. The energy of this band is the sum of two fundamental energies. If the "oscillation" of the mentioned terminal sulfate ligand (containing S5b) exhibits an external (rotational) mode, it could combine with the ν-(V═O) band of the nearby V1b atom. The energy of the external mode is around 250−350 cm^{-1} which is too low to be observed in the spectral range of Figure 4. Therefore, it is resonable to believe that the external mode could occur in a combination band with a sulfate mode, e.g., ν_3.

Thermogravimetry. The DTA curve (Figure 5) of the compound shows a temperature of fusion around 395 °C. The heat of fusion is an order of magnitude lower than expected for these types of compounds.[17] This is probably due to the large extent of glass formation during synthesis,

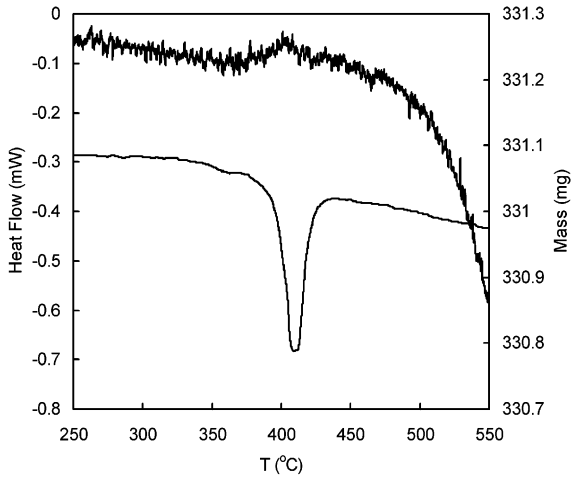

Figure 5. DTA and TGA curves of powder sample with stoichiometry corresponding to $K_8(VO)_2O(SO_4)_6$.

which is characteristic for compounds precipitated from vanadium−pyrosulfate−sulfate based melts. Probably 90% of the sample was glassy, as judged from DTA and visual observation in microscope. Due to the relatively fast scanning speed (5 °C/min), the TGA curve is not representing equilibrium at any given temperature. Still, it is seen from Figure 5 that decomposition of the compound starts already at the melting point around 400 °C. After the experiment, the sample contained green particles, a sign of formation of vanadium compounds in lower oxidation states. $K_8(VO)_2O(SO_4)_6$ is therefore probably not a dominant species in equilibrated vanadium−pyrosulfate−sulfate melts, since previous high temperature measurements[7,8] prove $VO_2(SO_4)_2^{3-}$ and $(VO)_2O(SO_4)_4^{4-}$ to be the dominant species at around 450−470 °C. However, at 400 °C, the compound may still

(16) Hardcastle, F. D.; Wachs, I. E. *J. Phys. Chem.* **1991**, *95*, 5034.

(17) Folkmann, G. E.; Hatem, G.; Fehrmann, R.; Gaune-Escard, M.; Bjerrum, N.-J. *Inorg. Chem.* **1993**, *32*, 1559.

partly lead to a stable dimeric complex in melts with high sulfate activity and relatively low vanadium content.

Relation to Catalysis. Even though the anion of this compound appears unstable in the molten phase, noteworthy information can be extracted by consideration of the structural properties of this compound compared to those present in the activated SO_2 oxidation catalyst. It is very interesting to see how the "two extra" ligands coordinate to the stable dimeric entity $(VO)_2O(SO_4)_4^{4-}$, believed[1] to be the catalytic active species in the molten salt catalyst. The V−O−S−O−V bridging in $(VO)_2O(SO_4)_6^{8-}$ is established by pushing away chelate bound sulfate in $(VO)_2O(SO_4)_4^{4-}$ so that the chelating sulfates become monodentate. In a less basic melt (as in the case of the activated catalyst), it is likely that SO_3 can react by the schemes

$$(VO)_2O(SO_4)_4^{4-} + 2SO_3 \rightarrow 2VO(SO_4)_2^{-} + S_2O_7^{2-} \quad (1)$$

or

$$(VO)_2O(SO_4)_4^{4-} + 2SO_3 \rightarrow (VO)_2O(SO_4)_2 + 2S_2O_7^{2-} \quad (2)$$

and possibly also to form $(VO)_2(SO_4)_3$ at high SO_3 partial pressures.

This could be unwanted side reactions in the last sequence of the catalytic cycle,[1,18] where SO_3, the product, leaves the catalyst. The compounds $MVO(SO_4)_2$ ($M = K^+$ or NH_4^+) have previously been prepared in SO_3 rich atmosphere yielding crystals suitable for structure determination by X-ray diffraction.[15] These structures exhibit no μ-oxo V−O−V bridge but a three-dimensional network of SO_4^{2-} groups, monodentate coordinated to different vanadium atoms. Therefore, the complex $VO(SO_4)_2^{-}$ or the polymeric form of this $(VO(SO_4)_2)_n^{n-}$ are possibly formed in the working catalyst at high SO_3 partial pressure. As already mentioned, the compound $(VO)_2O(SO_4)_2$ (sometimes formulated as $V_2O_3(SO_4)_2$) has been synthesized from V_2O_5 and SO_3 at high partial pressure of SO_3. At even higher SO_3 partial pressure, it can be imagined that a further oxide ion in V_2O_5 can react with SO_3 forming the possible species $(VO)_2(SO_4)_3$. As observed for $MVO(SO_4)_2$, the structure of $(VO)_2(SO_4)_3$ will most probably not contain the μ-oxo V−O−V bridge that seems to be essential for the O_2 activation which leads to the oxidation of SO_2 to SO_3. In the case of the formation of $(VO)_2O(SO_4)_2$, the reaction (eq 2) has changed the structure of the catalytic active species $(VO)_2O(SO_4)_4^{4-}$ to exhibit two bidentate bridging SO_4^{2-} groups in addition to the μ-oxo V−O−V bridge probably blocking the vanadium complex for coordination and activation of O_2.

This scenario for change of the complex formation in the catalyst at increased SO_3 partial pressure from active to inactive vanadium species is also in accordance with the negative reaction order reported from kinetic studies of the catalyst;[19] i.e., the presence of SO_3 leads to the blocking of sites in the active vanadium complex for the rate-limiting coordination of the O_2 molecule.[1] The apparent flexibility of the catalytic active species indicates thus that SO_3 can be formed from activated O and SO_2 and then link as a chelate sulfate ligand to each of the two VO_6 units.

Although speculative, new information on possible coordination of the active species has been obtained in the present work, allowing for the enlightening of more details of the catalytic cycle in the future.

Acknowledgment. NATO's Scientific Affairs Division in the framework of the Science for Pearce Programme (SfP 971984) and the Danish Natural Science and Technical Science Research Foundations are thanked for financial support.

Supporting Information Available: Crystallographic data in CIF-format. This material is available free of charge via the Internet at http://pubs.acs.org.

IC0301674

(18) Hatem, G.; Eriksen, K. M.; Gaune-Escard, M.; Fehrmann, R. *Topics Catal.* **2002**, *19* 323.

(19) Urbanek, A.; Trela, M. *Catal. Rev.—Sci. Eng.* **1980**, *21*, 73.